
Characterizing the Optimal $0 - 1$ Loss for Multi-class Classification with a Test-time Attacker

Sihui Dai^{*1} Wenxin Ding^{*2} Arjun Nitin Bhagoji² Daniel Cullina³ Ben Y. Zhao² Haitao Zheng²
Prateek Mittal¹

Abstract

Finding classifiers robust to adversarial examples is critical for their safe deployment. Determining the robustness of the best possible classifier under a given threat model for a given data distribution and comparing it to that achieved by state-of-the-art training methods is thus an important diagnostic tool. In this paper, we find achievable information-theoretic lower bounds on loss in the presence of a test-time attacker for *multi-class classifiers on any discrete dataset*. We provide a general framework for finding the optimal $0 - 1$ loss that revolves around the construction of a conflict hypergraph from the data and adversarial constraints. We further define other variants of the attacker-classifier game that determine the range of the optimal loss more efficiently than the full-fledged hypergraph construction. Our evaluation shows, for the first time, an analysis of the gap to optimal robustness for classifiers in the multi-class setting on benchmark datasets.

1. Introduction

Determining lower bounds on the robustness of classifiers to adversarial examples (Szegedy et al., 2013; Carlini & Wagner, 2016; Bhagoji et al., 2017) has emerged as an important problem to understand how effective specific classifiers are (Bunel et al., 2017; Tjeng et al., 2019; Goyal et al., 2018) as well as what non-trivial regimes for learning any binary classifier in the presence of adversarial examples are (Pydi & Jog, 2020; Bhagoji et al., 2019; 2021). Lower bounds have allowed a move away from the attack-defense arms race (Madry et al., 2018; Zhang et al., 2019; Croce & Hein,

2020) to a better understanding of how robust classifiers can be.

In this paper, we propose methods to find the optimal loss in the presence of a test-time attacker in the full multi-class setting, extending previous work which was restricted to the binary setting. This enables us to compare the robustness of multi-class classifiers used in practice to the optimal loss. Our **first contribution** is thus *extending the framework for computing lower bounds for robustness over all measurable functions to the multi-class setting*. In this framework, given a dataset and adversary, we construct a *conflict hypergraph* which contains vertices representing training examples in the dataset, and hyperedges representing overlaps between adversarial neighborhoods around each training example. Using this hypergraph, we construct a linear program whose optimal value is a lower bound on the $0 - 1$ loss for all classifiers and whose solution is the optimal classifier.

We further find that varying the information available to either the adversary or classifier leads to other optimization problems whose solutions are of independent interest. Since the full multi-class formulation of the lower bound, although exact, can lead to prohibitively large optimization problems in practice, we use these variants to find alternative valid bounds. Our **second contribution** is the *analysis of more efficient methods to determine the range of loss obtained by the optimal classifier and the interpretation of these bounds as the optimal losses for variations on the adversarial classification game* (see Table 1). In particular, we find lower bounds on the optimal loss by aggregating the set of all binary classifier-only lower bounds as well as by using truncated hypergraphs (hypergraphs with a restriction on the maximum hyperedge degree). We upper bound the optimal loss with a generalization of the Caro-Wei bound (Alon & Spencer, 2016) on a graph’s independent set size.

To analyze the performance of classifiers obtained from adversarial training (Madry et al., 2018; Zhang et al., 2019), we compare the loss obtained through adversarial training to that of the optimal classifier. We find a loss differential that is greatly exacerbated compared to the binary case (Bhagoji et al., 2019; Pydi & Jog, 2020). In addition, we also determine the cases where, in practice, the bounds obtained from

^{*}Equal contribution ¹Department of Electrical Engineering and Computer Science, Princeton University ²Department of Computer Science, University of Chicago ³Department of Electrical Engineering and Computer Science, Pennsylvania State University. Correspondence to: Sihui Dai <sihuid@princeton.edu>, Wenxin Ding <wenxind@uchicago.edu>.

	Summary of Method	Location
Optimal 0-1 loss	LP on conflict hypergraph	Section 2.3
Lower bounds for optimal 0-1 loss	LP on truncated conflict hypergraph	Section 3.1
	Combining binary classification bounds	Section 3.2
Upper bound for optimal 0-1 loss	Generalization of Caro-Wei bound	Section 3.3

Table 1: Summary of methods for obtaining computing optimal 0-1 loss and efficient bounds on this value.

game variants are close to the optimal. We find that while the aggregation of binary classifier-only bounds leads to a very loose lower bound, the use of truncated hyperedges can significantly speed up computation while achieving a loss value close to optimal. This is validated using the upper bound computed via bounding the size of the independent set, with the lower and upper bounds on the optimal loss closely matching for adversarial budgets used in practice. Thus, our **final contribution** is an *extensive empirical analysis of the behavior of the optimal loss for a given adversary, along with its lower and upper bounds*. This enables practitioners to utilize our methods even when the optimal loss is computationally challenging to determine.

The rest of the paper is organized as follows: §2 provides the characterization of the optimal loss; §3 proposes several upper and lower bounds on the optimal loss; §4 computes and compares the optimal loss to these bounds, as well as the performance of robustly trained classifiers and §5 concludes with a discussion of limitations and future work.

2. Characterizing Optimal 0-1 Loss

In this section, we provide a framework for obtaining the optimal 0 – 1 loss for any discrete distribution (*e.g.* training set) in the presence of a test-time adversary. We will show that this loss can be computed as the solution of a linear program (LP), which is defined based on a hypergraph constructed from the classification problem and attacker specification. We note that this loss is achievable, and is a *lower bound on the loss attainable by any classifier*.

2.1. Problem Formulation

Notation. We consider a supervised classification problem where inputs are sampled from input space \mathcal{X} , and labels belong to K classes: $y \in \mathcal{Y} = [K] = \{1, \dots, K\}$. Let P be the joint probability over $\mathcal{X} \times \mathcal{Y}$. Let $\mathcal{H}_{\text{soft}}$ denote the space of all soft classifiers; *i.e.* specifically, for all $h \in \mathcal{H}_{\text{soft}}$ we have that $h : \mathcal{X} \rightarrow [0, 1]^K$ and $\sum_{i=1}^K h(x)_i = 1$ for all $x \in \mathcal{X}$. Here, $h(x)_i$ represents the probability that the input x belongs to the i^{th} class. We use the natural extension of 0-1 loss, or equivalently classification error probability, to soft classifiers as our loss function: $\ell(h, (x, y)) = 1 - h(x)_y$.

This reduces to 0-1 loss when $h(x) \in \{0, 1\}^K$.¹

Test-time adversaries. We are interested in the setting where there exists a test-time adversary that can modify any data point x to generate an adversarial example \tilde{x} that lies within the neighborhood $N(x)$ of x . We require that for all $x \in \mathcal{X}$, $N(x)$ always contains x . The optimal loss, which depends on a distribution P , hypothesis class \mathcal{H} , and neighborhood N , is

$$\begin{aligned} L^*(P, N, \mathcal{H}) &= \inf_{h \in \mathcal{H}} \sup_{\tilde{x} \in N(x)} \ell(h, (\tilde{x}, y)) \\ &= 1 - \sup_{h \in \mathcal{H}} \inf_{\tilde{x} \in N(x)} h(\tilde{x})_y. \end{aligned} \quad (1)$$

Alternative hypothesis classes. In general, when $\mathcal{H}' \subseteq \mathcal{H}$, $L^*(P, N, \mathcal{H}) \leq L^*(P, N, \mathcal{H}')$. Two particular cases of this are relevant. First, the class of hard-decision classifiers is a subset of the class of soft classifiers ($\mathcal{H}_{\text{soft}}$). Second, for any fixed architecture, the class of functions represented by some parameterization of that architecture is another subset. Thus, optimal loss over $\mathcal{H}_{\text{soft}}$ provides a lower bound on loss for these settings.

2.2. Optimal loss for distributions with finite support

Since we would like to compute the optimal loss for distributions P with *finite support*, we can rewrite the expectation in Equation 1 as an inner product. Let V be the support of P , *i.e.* the set of points $(x, y) \in \mathcal{X} \times \mathcal{Y}$ that have positive probability in P . Let $p \in [0, 1]^V$ be the probability mass vector for P : $p_v = P(\{v\})$. For a soft classifier h , let $q_N(h) \in \mathbb{R}^V$ be the vector of correct classification probabilities for vertices $v = (x, y) \in V$, *i.e.* $q_N(h)_v := \inf_{\tilde{x} \in N(x)} h(\tilde{x})_y$. Rewriting (1) with our new notation, we have $1 - L^*(P, \mathcal{H}_{\text{soft}}, N) = \sup_{h \in \mathcal{H}_{\text{soft}}} p^T q_N(h)$. This is the maximization of a linear function over all possible vectors $q_N(h)$. In fact, the convex hull of all correct classification probability vectors is a polytope and this optimization problem is a linear program, as described next.

Definition 2.1. For a soft classifier h , the correct-classification probability achieved on an example $v =$

¹A soft classifier can be interpreted as a randomized hard-decision classifier f with $\Pr[f(x) = y] = h(\tilde{x})_y$, in which case $\ell(h, (x, y)) = \Pr[f(x) \neq y]$, classification error probability of this randomized classifier.

(x, y) in the presence of an adversary with constraint N is $q_N(h)_v = \inf_{\tilde{x} \in N(x)} h(\tilde{x})_y$.

The space of achievable correct classification probabilities is $\mathcal{P}_{\mathcal{V}, N, \mathcal{H}} \subseteq [0, 1]^{\mathcal{V}}$, defined as

$$\mathcal{P}_{\mathcal{V}, N, \mathcal{H}} = \bigcup_{h \in \mathcal{H}} \prod_{v \in \mathcal{V}} [0, q_N(h)_v]$$

In other words we say that $q' \in [0, 1]^{\mathcal{V}}$ is feasible when there exists $h \in \mathcal{H}$ such that $q' \leq q_N(h)$. The inequality appears because we will always take nonnegative linear combinations of correct classification probabilities.

Characterizing $\mathcal{P}_{\mathcal{V}, N, \mathcal{H}}$ allows the minimum adversarial loss achievable to be expressed as an optimization problem with a linear objective:²

$$\sup_{h \in \mathcal{H}_{\text{soft}}} p^T q_N(h) = \sup_{q \in \mathcal{P}_{\mathcal{V}, N, \mathcal{H}}} \sum_{v \in \mathcal{V}} p_v q_v. \quad (2)$$

(Bhagoji et al., 2021) characterized $\mathcal{P}_{\mathcal{V}, N, \mathcal{H}_{\text{soft}}}$ in the two-class case and demonstrated that this space can be captured by linear inequalities. We now demonstrate that this also holds for the multi-class setting.

2.3. Linear Program to obtain Optimal Loss

In order to characterize $\mathcal{P}_{\mathcal{V}, N, \mathcal{H}_{\text{soft}}}$, we represent the structure of the classification problem with a *conflict hypergraph* $\mathcal{G}_{\mathcal{V}, N} = (\mathcal{V}, \mathcal{E})$, which records intersections between neighborhoods of points in \mathcal{X} . The set of vertices \mathcal{V} of $\mathcal{G}_{\mathcal{V}, N}$ is the support of P . \mathcal{E} denotes the set of hyperedges of the graph. For a set $S \subseteq \mathcal{V}$, $S \in \mathcal{E}$ (i.e. S is a hyperedge in $\mathcal{G}_{\mathcal{V}, N}$) if all vertices in S belong to different classes and the neighborhoods of all vertices in S overlap: $\bigcap_{(x, y) \in S} N(x) \neq \emptyset$. Thus, the size of each hyperedge is at most K , \mathcal{E} is downward-closed, and every $v \in \mathcal{V}$ is a degree 1 hyperedge.

Using the conflict hypergraph $\mathcal{G}_{\mathcal{V}, N}$, we can now describe $\mathcal{P}_{\mathcal{V}, N, \mathcal{H}_{\text{soft}}}$.

Lemma 2.2 (Feasible output probabilities (Adapted from (Bhagoji et al., 2021))). *The set of correct classification probability vectors for support points \mathcal{V} , adversarial constraint N , and hypothesis class $\mathcal{H}_{\text{soft}}$ is*

$$\mathcal{P}_{\mathcal{V}, N, \mathcal{H}_{\text{soft}}} = \{q \in \mathbb{R}^{\mathcal{V}} : q \geq \mathbf{0}, Bq \leq \mathbf{1}\} \quad (3)$$

where $B \in \mathbb{R}^{\mathcal{E} \times \mathcal{V}}$ is the edge incidence matrix of the conflict graph $\mathcal{G}_{\mathcal{V}, N}$.

See Appendix A for proof.

²For any loss function that is a decreasing function of $h(\tilde{x})_y$, the optimal loss can be specified as an optimization over $\mathcal{P}_{\mathcal{V}, N, \mathcal{H}}$. In fact (Bhagoji et al., 2021) focused on cross-entropy loss, which has this property.

Then, using this feasible region as a constraint in our optimization problem in Equation 2, we arrive at the following:

Corollary 2.3 (Optimal loss as an LP). *For any distribution P with finite support,*

$$1 - L^*(P, N, \mathcal{H}_{\text{soft}}) = \max_q p^T q \text{ s.t. } q \geq 0, Bq \leq \mathbf{1}. \quad (4)$$

Corollary 2.3 allows us to compute optimal loss via LP for any dataset and adversary.

Duality and adversarial strategies. The dual linear program is

$$\min_z \mathbf{1}^T z \text{ s.t. } z \geq 0, B^T z \geq p.$$

Feasible points in the dual linear program are fractional coverings of the vertices by the hyperedges. Optimal coverings can be interpreted as adversarial strategies. For each hyperedge e , there is an example \tilde{x} such that $\tilde{x} \in N(x)$ for each $(x, y) \in e$. When the adversary samples the natural example V , it can select the hyper edge E to generate the adversarial example using any condition distribution that satisfies $\Pr[E = e | V = v] \leq \frac{B_{e,v} z_e}{p_v}$. Note that $B_{e,v} z_e$ is the amount of coverage of v coming from e and $\sum_e B_{e,v} z_e = (B^T z)_v \geq p_v$. Thus for a vertex v such that $(B^T z)_v = p_v$, there is only one choice for this distribution. For a vertex v that is over-covered, i.e. $(B^T z)_v > p_v$, the adversary has some flexibility. For over-covered vertices, by complementary slackness $q_v = 0$ in every optimal q , so the optimal classifiers do not attempt to classify v correctly.

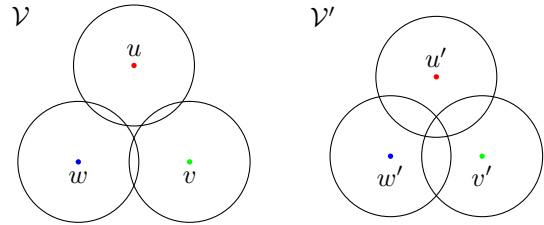


Figure 1: Two possible conflict structures involving three examples, each from a different class. In the right case, all subsets of $\mathcal{V}' = \{u', v', w'\}$ are hyperedges in the conflict hypergraph $\mathcal{G}_{\mathcal{V}', N}$. In the left case, $\{u, v, w\}$ is not a hyperedge in $\mathcal{G}_{\mathcal{V}, N}$, but all other subsets of \mathcal{V} are.

Three-class minimal examples. Corollary 2.3 demonstrates that the optimal loss for the multi-class problem is influenced by hyperedges between vertices which reflect higher order interactions between examples. Figure 1 shows an important distinction between two types of three-way interactions of examples.

In case one, $L^*(P, \mathcal{H}_{\text{soft}}, N) = \max(p_u, p_v, p_w, \frac{1}{2})$. In case two, $L^*(P', \mathcal{H}_{\text{soft}}, N) = \max(p'_u, p'_v, p'_w)$. The presence or absence of the size-three hyperedge affects the

optimal loss when the example probabilities are close to balanced, i.e. all at most $\frac{1}{2}$.

It is instructive to consider the optimal classifiers and adversarial strategies in the two cases. For \mathcal{V} , when $\frac{1}{2} \leq p_u$, the classifier that returns $(1, 0, 0)$ everywhere is optimal. The optimal cover satisfies $z_{\{u,v\}} + z_{\{u,w\}} = p_u$, $z_{\{u,v\}} \geq p_v$, $z_{\{u,w\}} \geq p_w$, $z_{\{v,w\}} = 0$. Thus when the adversary samples v or w , it always produces an adversarial example that could be confused for u . When $\max(p_u, p_v, p_w) \leq \frac{1}{2}$, the classifier that returns $(\frac{1}{2}, \frac{1}{2}, \frac{1}{2})$ everywhere is optimal. The cover $z_{\{u,v\}} = p_u + p_v - \frac{1}{2}$, $z_{\{u,w\}} = p_u + p_w - \frac{1}{2}$, and $z_{\{v,w\}} = p_v + p_w - \frac{1}{2}$ is optimal and has cost $\frac{1}{2}$. The adversary produces examples associated with all three edges.

For \mathcal{V}' , things are simpler. The cover $z_{\{u,v,w\}} = \max(p_u, p_v, p_w)$ is always optimal. When $p_u \geq \max(p_v, p_w)$, the classifier that returns $(1, 0, 0)$ everywhere is optimal.

2.4. Optimal Loss for Hard Classifiers

A hard classifier $h : \mathcal{X} \rightarrow \{0, 1\}^{[K]}$ has 0, 1-valued correct classification probabilities. When we apply the classifier construction procedure from the proof of Lemma 2.2 using an integer-valued q vector, we obtain a hard classifier. Thus the possible correct classification probabilities for hard classifiers are $\mathcal{P}_{\mathcal{V},N,\mathcal{H}_{soft}} \cap \{0, 1\}^{[K]}$. These are exactly the indicator vectors for the independent sets in the graph on \mathcal{V} formed by the hyperedges of size two in $\mathcal{G}_{\mathcal{V},N}$: the vertices included in the independent set are classified correctly and the remainder are not. Formally, we can express hard classifier loss as:

$$\begin{aligned} & 1 - L^*(P, N, \mathcal{H}_{hard}) \\ &= \max_q p^T q \text{ s.t. } q \in \{0, 1\}, Bq \leq 1. \\ &= \max_q p^T q \text{ s.t. } q \in \{0, 1\}, B^{\leq 2} q \leq 1. \\ &= \max_{S \subseteq \mathcal{V}: S \text{ independent in } \mathcal{G}^{\leq 2}} P(S). \end{aligned}$$

Finding the maximum weight independent set is an NP hard problem, which makes it computationally inefficient to compute optimal hard classifier loss. In Section 3, we will discuss how to obtain an upper bound on $L^*(P, N, \mathcal{H}_{hard})$ and other truncations of $\mathcal{G}_{\mathcal{V},N}$.

2.5. Two-class versus Multi-class hard classification

Now we can summarize the relationships between the two-class and multi-class settings. The facts mentioned in this section are all well-known in graph and hypergraph theory. We interpret their consequences for adversarial classification.

When $K = 2$, the conflict hypergraph is a bipartite graph. For bipartite graphs, three different polytopes coincide:

- The independent set polytope, which is the convex hull of the independent set indicators.
- The fractional independent set polytope, which has a constraint $\sum_{i \in S} q_i \leq 1$ for each clique S .
- The fractional vertex packing polytope, which has a constraint $\sum_{i \in e} q_i \leq 1$ for each edge e .

Due to this, in the two class setting, $\mathcal{P}_{\mathcal{V},N,\mathcal{H}_{soft}}$ is the convex hull of $\mathcal{P}_{\mathcal{V},N,\mathcal{H}_{hard}}$, hard classifiers achieve the optimal loss, and optimal hard classifiers can be found efficiently.

For $K > 2$, all of these concepts become distinct. An independent set in a hypergraph is a subset of vertices that induces no hyperedges. In other words, a hyperedge of size m must contain at most $m - 1$ vertices from an independent set. Because the conflict hypergraph is hereditary, only the size-two hyperedges provide binding constraints. Thus the concept of a hypergraph independent set is not truly relevant for our application.

As seen in Lemma 2.2, the fractional vertex packing polytope characterizes performance in soft classification problem. The fractional independent set polytope of $\mathcal{G}^{\leq 2}$ has no particular significance. Every hyperedge in \mathcal{G} produces a clique in $\mathcal{G}^{\leq 2}$ but not the reverse.

Furthermore, when $K > 2$ the fractional vertex packing polytope of the conflict hypergraph, i.e. $\mathcal{P}_{\mathcal{V},N,\mathcal{H}_{soft}}$, can have non-integral extreme points. This means it can be strictly larger than the independent set polytope. The first configuration in Figure 1 illustrates this. Thus the soft and hard classification problems involve optimization over different spaces of correct classification probabilities. Furthermore, maximum weight or even approximately maximum weight independent sets cannot be efficiently found in general graphs: the independent set polytope is not easy to optimize over.

In Section 3.3, we will use an efficiently computable lower bound on the independence number of a graph.

3. Bounds on Optimal 0-1 Loss

While Lemma 2.3 characterizes the optimal loss, it may be computationally expensive to construct conflict hypergraphs in practice for a given dataset and to solve the linear program. Thus, we discuss several methods of bounding the optimal loss from the LP in Lemma 2.3, which are computationally faster in practice (§4.2).

3.1. Lower bounds on multiclass optimal loss via truncated hypergraphs

The edge set of the hypergraph \mathcal{G} could be very large: there are $\prod_{i \in [K]} (1 + |V_i|)$ vertex sets that are potential hyperedges. Even when the edge set is reasonable, it is not

clear that higher order hyperedges can be computed from \mathcal{V} efficiently. To work around these issues, we consider the truncated hypergraphs with bounded size hyperedges: $\mathcal{G}^{\leq m} = (\mathcal{V}, \mathcal{E}^{\leq m})$ where $\mathcal{E}^{\leq m} = \{e \in \mathcal{E} : |e| \leq m\}$. In the corresponding relaxation of (4), B is replaced by $B^{\leq m}$, the incidence matrix for $\mathcal{E}^{\leq m}$. Since $\mathcal{E}^{\leq m} \subseteq \mathcal{E}$, this relaxation provides a lower bound on $L^*(P, N, \mathcal{H}_{\text{soft}})$.

Classification with side-information. This relaxation has an interpretation as the optimal loss in a variation of the classification game with side information. In the example-dependent class list game with list length m , the adversary samples $(x, y) \sim P$, then selects \tilde{x} and $C \subseteq \mathcal{Y}$ such that $y \in C$ and $|C| = m$. The classifier receives both \tilde{x} and C , so the classifier is a function $h : \mathcal{X} \times \binom{\mathcal{Y}}{m} \rightarrow \mathcal{Y}$, where $\binom{\mathcal{Y}}{m}$ is the set of m -element subsets of \mathcal{Y} . We call C the side information. Let $L^*(m, P, \mathcal{H}, N) =$ be the minimum loss in this game.

To illustrate this, consider the distribution P' from Figure 1 with $m = 2$. The adversary can select some $\tilde{x} \in N(u') \cap N(v') \cap N(w')$, but the classifier will use the side-information to eliminate one of the three classes. The classifier is in the same situation it would be if the distribution were P and the size-three hyperedge was absent.

For classifiers using class list side-information, the correct classification probability is defined as follows: $q_{m,N}(h)_{(x,y)} = \inf_{\tilde{x} \in N(x)} \min_{C \in \binom{[K]}{m} : y \in C} h(\tilde{x}, C)_y$. When $m = K$, the minimization over C is trivial and this reduces to our previous definition of $q_N(h)$.

Lemma 3.1 (Feasible output probabilities in the side-information game). *The set of correct classification probability vectors for side-information of size m , support points \mathcal{V} , adversarial constraint N , and hypothesis class $\mathcal{H}_{\text{soft}}$ is*

$$\mathcal{P}_{m,\mathcal{V},N,\mathcal{H}_{\text{soft}}} = \{q \in \mathbb{R}^{\mathcal{V}} : q \geq \mathbf{0}, B^{\leq m} q \leq \mathbf{1}\} \quad (5)$$

where $B^{\leq m} \in \mathbb{R}^{\mathcal{E}^{\leq m} \times \mathcal{V}}$ is the edge incidence matrix of the conflict graph $G_{\mathcal{V},N}^{\leq m}$.

The proof can be found in Appendix A.

Using the feasible correct classification probabilities in Lemma 3.1, we can now write the LP for obtaining the optimal loss for classification with side-information:

Corollary 3.2 (Optimal loss for classification with side information/ truncated hypergraph lower bound).

$$1 - L^*(P, N, \mathcal{H}_{\text{soft}}) = \max_q p^T q \quad \text{s.t. } q \geq \mathbf{0}, B^{\leq m} q \leq \mathbf{1}.$$

3.2. Lower bounds on multiclass optimal loss via lower bounds for binary classification

For large training datasets and large perturbation sizes, it may still be computationally expensive to compute lower

bounds via LP even when using truncated hypergraphs due to the large number of edge constraints. Prior works (Bhagoji et al., 2019; 2021) proposed methods of computing lower bounds for 0-1 loss for binary classification problems and demonstrate that their algorithm is more efficient than generic LP solvers. We now ask the question: *Can we use lower bounds for binary classification to efficiently compute a lower bound for multi-class classification?*

Consider the setting where we obtain the optimal 0 – 1 loss for all one-versus-one binary classification tasks. Specifically, for each $C \in \binom{[K]}{2}$, the binary classification task for that class pair uses example distribution $P|Y \in C$ and the corresponding optimal loss is $L^*((P|Y \in C), N, \mathcal{H}_{\text{soft}})$. What can we say about $L^*(P, N, \mathcal{H}_{\text{soft}})$ given these $\binom{K}{2}$ numbers?

This question turns about to be related to another variation of classification with side information that we call the *class-only side-information* game. The adversary samples $y \sim P_y$, then selects $C \in \binom{[K]}{m}$, then samples $x \sim P_{x|y}$ and selects $\tilde{x} \in N(x)$.

In the side information game from § 3.1, which we call the "example-dependent side-information" game, the adversary's choice of C can depend on both x and y . In the class-only variation it can only depend on y . Let $L_{\text{co}}^*(m, P, \mathcal{H}, N)$ be the minimum loss in the class-only class list game. For the class only game, we will focus on the $m = 2$ case.

To make the connection to the binary games, we need to add one more restriction on the adversary's choice of side information: for all y, y' $\Pr[C = y, y'|Y = y] = \Pr[C = y, y'|Y = y']$. This ensures that the classifier's posterior for Y given C is $\Pr[Y = y|C] = \Pr[Y = y]/\Pr[Y \in C]$.

Lemma 3.3. *The optimal loss in the class-only side-information game is*

$$L_{\text{co}}^*(2, P, N, \mathcal{H}) = \max_s \sum_{i,j} \Pr[Y = i] a_{i,j} s_{i,j}$$

where $a_{i,j} = L^*(P|(y \in \{i, j\}), \mathcal{H}, N)$ and $s \in \mathbb{R}^{[K] \times [K]}$ is a symmetric doubly stochastic matrix: $s \geq \mathbf{0}$, $s = s^T$, $s\mathbf{1} = \mathbf{1}$.

The proof in is Appendix A. The variable s represents the attacker's strategy for selecting the class side information. When the classes are equally likely, this optimization becomes a maximum weight coupling problem: because the weights a are symmetric, the constraint that s be symmetric becomes irrelevant.

3.3. Upper bounds on hard classifier loss via Caro-Wei bound on independent set probability

In §3.1 and 3.2, we discussed 2 ways of obtaining lower bounds for the loss of soft classifiers for the multi-class

classification problem. In this section, we provide an upper bound on the loss of the optimal hard classifier (we note that this is also an upper bound for optimal loss for soft classifiers). In §2.4, we discussed the relationship between optimal loss achievable by hard classifiers and independent set size. We upper bound the optimal loss of hard classifiers by providing a lower bound on the probability of independent set in the conflict graph.

The following lemma is a generalization of the Caro-Wei theorem (Alon & Spencer, 2016) and gives a lower bound on the weight of the maximum weight independent set.

Lemma 3.4. *Let \mathcal{G} be a graph on \mathcal{V} with adjacency matrix $A \in \{0, 1\}^{\mathcal{V} \times \mathcal{V}}$ and let P be a probability distribution on \mathcal{V} . For any nonnegative vertex weights $w \in \mathbb{R}^{\mathcal{V}}$, $w \geq 0$, there is some independent set $S \subseteq \mathcal{V}$ with*

$$P(S) \geq \sum_{v \in \mathcal{V}: w_v > 0} p_v \frac{w_v}{((A + I)w)_v}. \quad (6)$$

The proof is in Appendix A. Note that if w is the indicator vector for an independent set S' , the bound becomes $p^T w = P(S')$. In general, Lemma 3.4 can be thought of as a randomized procedure for rounding an arbitrary vector into an independent set indicator vector. Vectors w that are nearly independent set indicators yield better bounds.

Lemma 3.4 provides a lower bound on the size of the maximum independent set in $\mathcal{G}^{\leq 2}$ and thus an upper bound on $L^*(P, n, \mathcal{H}_{hard})$, which we call $L_{CW} = 1 - P(S)$.

3.4. Relationship between bounds

When $m = K$, $C = \mathcal{Y}$ and both the example-dependent and class-only side information games are equivalent to the original game, so $L^*(P, N, \mathcal{H}) = L^*(K, P, N, \mathcal{H}) = L_{co}^*(K, P, N, \mathcal{H})$. For each variation of the side-information game, the game becomes more favorable for the adversary as m increases: $L^*(m, P, n, \mathcal{H}) \leq L^*(m+1, P, N, \mathcal{H})$ and $L_{co}^*(m, P, N, \mathcal{H}) \leq L_{co}^*(m+1, P, N, \mathcal{H})$. For each m , it is more favorable for the adversary to see x before selecting C , i.e. $L_{co}^*(m, P, N, \mathcal{H}) \leq L^*(m, P, N, \mathcal{H})$.

We fix a choice of P and N and suppress them from our notation in the following inequalities:

$$\begin{aligned} 0 &= L_{co}^*(1, \mathcal{H}_{soft}) = L^*(1, \mathcal{H}_{soft}) \\ &\leq L_{co}^*(2, \mathcal{H}_{soft}) \leq L^*(2, \mathcal{H}_{soft}) \\ &\leq L^*(3, \mathcal{H}_{soft}) \\ &\leq \dots \leq L^*(K, \mathcal{H}_{soft}) = L^*(\mathcal{H}_{soft}) \\ &\leq L^*(\mathcal{H}_{hard}) \\ &\leq L_{CW} \end{aligned}$$

4. Empirical Results

In this section, we first find the optimal losses for 3-class problems with an ℓ_2 -constrained attacker (Goodfellow et al., 2015) and compare them to the loss of adversarially trained classifiers. We then compare the optimal loss in the 10-class setting to its upper and lower bounds (§3.4), showing matching bounds at lower ϵ . Hyperedge finding is detailed in Appendix B and the experimental setup in Appendix C.

4.1. Optimal loss for 3-way classification problems

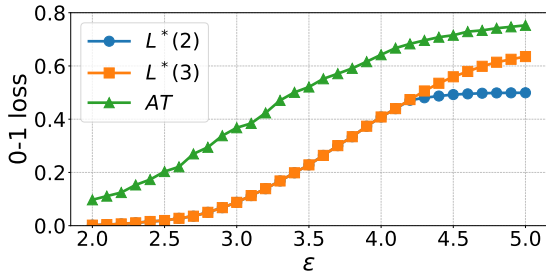
Lemma 2.3 allows us to compute the optimal loss given any dataset (and its corresponding conflict hypergraph). We begin with computing the optimal loss for 3-way classification problems, due to the computational complexity of finding higher order hyperedges (see Appendix D.4). In Figure 2, we plot the optimal loss $L^*(3)$ computed via the LP in Lemma 2.3 against the loss obtained through TRADES adversarial training (Zhang et al., 2019) for 3-class MNIST (classes 1, 4, 7) and 3-class CIFAR-10 (classes 0, 2, 8 which correspond to plane, bird, and ship respectively) with 1000 samples per class³. For MNIST, we train a 3 layer CNN for 20 epochs with TRADES regularization strength $\beta = 1$ and for CIFAR-10, we train a WRN-28-10 model for 100 epochs with $\beta = 6$. We evaluate models using APGD-CE from AutoAttack (Croce & Hein, 2020). Additional results for a mixture of 3 Gaussians are in Appendix D.1.

Since the optimal loss is over the space of all soft classifiers while the trained models are members of a smaller hypothesis class, we expect some gap in performance between adversarial training and our computed bounds. From Figure 2, we observe a large gap in performance of adversarial training in comparison to the computed optimal loss $L^*(3)$. In fact, we find that for CIFAR-10, adversarial training is unable to achieve loss much better than 0.6 at ϵ for which the optimal loss is near 0. This gap is much larger than observed by prior work (Bhagoji et al., 2019; 2021) for binary classification, suggesting that *current robust training techniques struggle more to fit training data with more classes*.

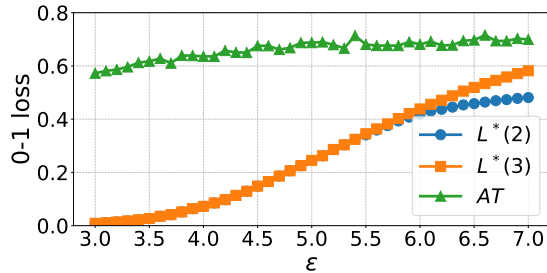
4.2. Bounds on optimal loss for 10-way classification

As the number of classes and dataset size increases, the difficulty of solving the LP in Lemma 2.3 increases. In this section, we use methods discussed in Section 3 in order to give a bound on the optimal loss for 10-way classification on MNIST and CIFAR-10 datasets on the full training dataset. We present results for each approximation in Figure 3. We note that for some methods, we are only able to obtain results up to a small value of ϵ due to blowup in runtime (See Appendix D.5 for details). We provide truncated hypergraph

³We also used PGD adversarial training (Madry et al., 2018) but found its performance to be far worse. (See Appendix D.2)

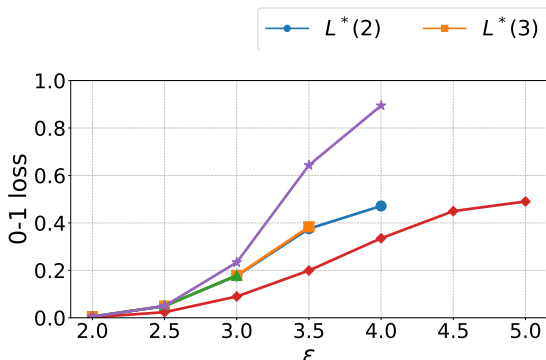


(a) MNIST (1,4,7)

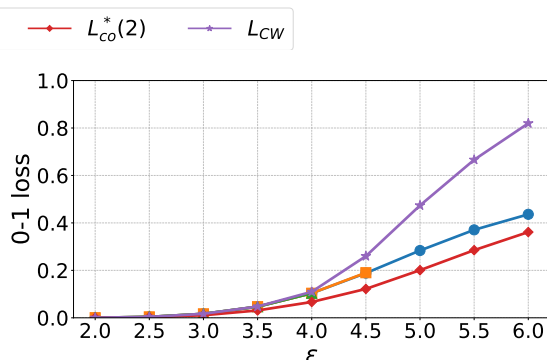


(b) CIFAR-10 (0,2,8)

Figure 2: Optimal error for MNIST and CIFAR-10 3-class problems ($L^*(3)$). $L^*(2)$ is a lower bound computed using only constraints from edges ($L^*(2)$). AT is the loss for a robust classifier under the strong APGD attack (Croce & Hein, 2020)



(a) MNIST



(b) CIFAR-10

Figure 3: Lower bounds on the exact optimal 10-class loss using hyperedges up to degree 2 ($L^*(2)$), 3 ($L^*(3)$) and 4 ($L^*(4)$), as well as maximum weight coupling of pairs of binary 0 – 1 loss lower bounds ($L_{co}^*(2)$). L_{CW} is an upper bound from the Caro-Wei approximation of the independent set number.

bounds for CIFAR-100 in Appendix D.3.

Lower bounds from truncated hypergraphs (§3.1): In Figure 3, we plot the loss lower bound obtained via by truncating the hypergraph to consider only edges ($L^*(2)$), up to degree 3 hyperedges ($L^*(3)$), and up to degree 4 hyperedges ($L^*(4)$). Interestingly, we find at small values of ϵ , there is little difference in these bounds despite the presence of many higher degree hyperedges. For example, for CIFAR-10 at $\epsilon = 3$, we observe 3M degree 3 hyperedges and 10M degree 4 hyperedges, but these edge constraints have no impact on the computed lower bound. We provide the count of hyperedges for each value of ϵ in Appendix D.4. In fact, from Figures 6 and 2, we find that the difference $L^*(2)$ and $L^*(3)$ does not occur until the loss reaches above 0.4 for the 3-way classification problem.

Takeaway: In practice, we *do not lose information from computing lower bounds with only edges in the conflict hypergraph.*

To understand why including more information about hyperedges does not influence the computed lower bound by

much, we examine the optimal classification probability q_v of each vertex obtained as a solution to the LP with ($L^*(3)$) and without considering constraints from degree 3 hyperedges ($L^*(2)$). Figure 4 contains a histogram of the distributions of q_v for MNIST. (A corresponding Figure for CIFAR-10 is in Appendix D.4.) For small ϵ , there is no change in the distribution of q_v , which results in no change in overall loss. For example, for MNIST at $\epsilon = 2.5$, we observe that the distribution of q_v stays the same between $L^*(2)$ and $L^*(3)$. However at larger values of ϵ , we find that for $L^*(2)$, more values are assigned q_v near 0.5, and these probabilities are highly impacted after incorporating hyperedge constraints. Because the values $L^*(2)$ and $L^*(3)$ are not significantly different, very few of the 0.5 values in the $L^*(2)$ solution were in triangles of $\mathcal{G}^{\leq 2}$ that were replaced by a hyperedge in $\mathcal{G}^{\leq 3}$.

Lower bounds from 1v1 binary classification problems (§3.2): In Section 3.2, we introduced a way to compute lower bounds on loss based on lower bounds for binary classification problems. Since classes are equally likely for our datasets, we use maximum weight coupling over

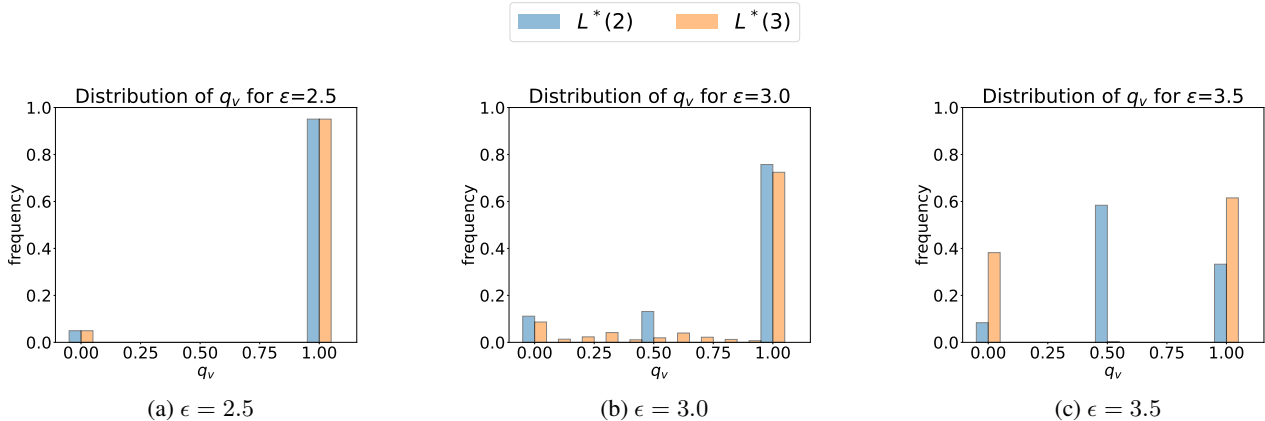


Figure 4: Distribution of optimal classification probabilities q obtained by solving the LP with up to degree 2 hyperedges ($m = 2$) and up to degree 3 hyperedges ($m = 3$) on the MNIST training set.

the optimal losses for all pairs of 1v1 binary classification problems. We provide heat maps of the optimal loss for each pair of classes in MNIST and CIFAR-10 in Appendix D.6. Since Bhagoji et al. (2021) introduce an algorithm for efficiently computing lower bounds for binary classification, this technique can be more efficient than using truncated hypergraphs, allowing us to compute lower bounds at larger values of ϵ in Figure 3. However, we note that this technique scales poorly as the number of classes K increases due to the need for computing lower bounds for all $\binom{K}{2}$ pairs of binary classification problems.

Takeaway: From Figure 3, we find that *while this lower bound is the most efficient to compute, the obtained bound is much looser compared to that from truncated hypergraphs.*

Upper bounding optimal loss via Caro-Wei (§3.3): From Figure 3, we also plot the upper bound on 0-1 loss for hard classifiers (denoted by $L^*(\mathcal{H}_{\text{hard}})$) obtained via applying Lemma 3.4 with vertex weights obtained from the solution to $L^*(2)$. When ϵ becomes large ($\epsilon \geq 3.0$ for MNIST and $\epsilon \geq 4.5$ for CIFAR-10), we find that the upper bound on loss blows up, which suggests that at larger values of ϵ higher order interactions matter more. However, these values of ϵ are much larger than studied in practice. We observe that at small values of ϵ (achieving less than 0.2 error), the lower bounds obtained through truncated hypergraphs ($L^*(2)$, $L^*(3)$, and $L^*(4)$) are close to the value of this upper bound. Also, $L^*(\mathcal{H}_{\text{hard}})$ is also an upper bound on hard classifier 0-1 loss,

Takeaways: (i) *We do not lose much information from not including all hyperedges at small ϵ values;* (ii) *At these small values of ϵ , we do not expect much difference in performance between hard classifiers and soft classifiers.*

5. Discussion and Related Work

Related Work: When the data distribution satisfies certain properties, (Dohmatob, 2019) and (Mahloujifar et al., 2019) use the ‘blowup’ property to determine bounds on the robust loss, given some level of loss on benign data. We note that these papers use a different loss function that depends on the original classification output on benign data, thus their bounds are not comparable. (Bhagoji et al., 2019), (Pydi & Jog, 2020) and (Bhagoji et al., 2021) provide lower bounds on robust loss when the set of classifiers under consideration is all measurable functions. These bounds are classifier-agnostic and do not depend on the loss on benign data. All of these papers only provide bounds in the binary classification setting. The closest related work to our is (Trillos et al., 2023), which uses optimal transport theory to find lower bounds on multi-class classification. However, they do not grapple with the computational bottlenecks for larger class sizes and only obtain approximate bounds.

Discussion and Limitations: Our work in this paper firmly establishes for the multi-class case what was known only in the binary setting before: *there exists a large gap in the performance of current robust classifiers and the optimal classifier.* This raises the question: *why does this gap arise and how can we improve training to decrease this gap?* It also provides methods to bound the loss efficiently in practice, giving practitioners quick means to determine the gap. This paper, however, does not tackle the problem of actually closing this gap. Possible methods include increasing the architecture size (Sehwag et al., 2022), using additional data (Gowal et al., 2021) and using soft-labels (Bhagoji et al., 2021). A surprising finding from our experiments was that the addition of hyperedges to the multi-way conflict graph did not change the lower bounds much, indicating we are in a regime where multi-way intersections minimally impact optimal probabilities. One major limitation of our work is

the computational expense at larger budgets, sample sizes and class sizes. We suspect this is due to the general-purpose nature of the solvers we use and future work should look into developing custom algorithms to speed up the determination of lower bounds.

References

- Alon, N. and Spencer, J. H. *The probabilistic method*. John Wiley & Sons, 2016.
- Andersen, M. S., Dahl, J., and Vandenberghe, L. Cvxopt: Python software for convex optimization, 2013.
- ApS, M. *MOSEK Optimizer API for Python 10.0.22*, 2019. URL <https://docs.mosek.com/10.0/pythonapi/index.html>.
- Bhagoji, A. N., He, W., Li, B., and Song, D. Exploring the space of black-box attacks on deep neural networks. *arXiv preprint arXiv:1712.09491*, 2017.
- Bhagoji, A. N., Cullina, D., and Mittal, P. Lower bounds on adversarial robustness from optimal transport. In *Advances in Neural Information Processing Systems*, pp. 7496–7508, 2019.
- Bhagoji, A. N., Cullina, D., Sehwas, V., and Mittal, P. Lower bounds on cross-entropy loss in the presence of test-time adversaries. In *Proceedings of the 38th International Conference on Machine Learning*, 2021.
- Bunel, R., Turkaslan, I., Torr, P. H., Kohli, P., and Kumar, M. P. A unified view of piecewise linear neural network verification. *arXiv preprint arXiv:1711.00455*, 2017.
- Carlini, N. and Wagner, D. A. Towards evaluating the robustness of neural networks. *CoRR*, abs/1608.04644, 2016. URL <http://arxiv.org/abs/1608.04644>.
- Croce, F. and Hein, M. Reliable evaluation of adversarial robustness with an ensemble of diverse parameter-free attacks. In *International Conference on Machine Learning*, pp. 2206–2216. PMLR, 2020.
- Dohmatob, E. Generalized no free lunch theorem for adversarial robustness. In *Proceedings of the 36th International Conference on Machine Learning*, pp. 1646–1654, 2019.
- Goodfellow, I. J., Shlens, J., and Szegedy, C. Explaining and harnessing adversarial examples. In *International Conference on Learning Representations*, 2015.
- Gowal, S., Dvijotham, K., Stanforth, R., Bunel, R., Qin, C., Uesato, J., Mann, T., and Kohli, P. On the effectiveness of interval bound propagation for training verifiably robust models. *arXiv preprint arXiv:1810.12715*, 2018.
- Gowal, S., Qin, C., Uesato, J., Mann, T., and Kohli, P. Uncovering the limits of adversarial training against norm-bounded adversarial examples. *arXiv preprint arXiv:2010.03593*, 2020.
- Gowal, S., Rebuffi, S., Wiles, O., Stimberg, F., Calian, D. A., and Mann, T. A. Improving robustness using generated data. In Ranzato, M., Beygelzimer, A., Dauphin, Y. N., Liang, P., and Vaughan, J. W. (eds.), *Advances in Neural Information Processing Systems 34: Annual Conference on Neural Information Processing Systems 2021, NeurIPS 2021, December 6-14, 2021, virtual*, pp. 4218–4233, 2021. URL <https://proceedings.neurips.cc/paper/2021/hash/21ca6d0cf2f25c4dbb35d8dc0b679c3f-Abstract.html>.
- Huang, L., Joseph, A. D., Nelson, B., Rubinstein, B. I., and Tygar, J. Adversarial machine learning. In *Proceedings of the 4th ACM workshop on Security and Artificial Intelligence*, pp. 43–58. ACM, 2011.
- Krizhevsky, A. and Hinton, G. Learning multiple layers of features from tiny images. 2009.
- LeCun, Y. and Cortes, C. The MNIST database of handwritten digits. 1998.
- Madry, A., Makelov, A., Schmidt, L., Tsipras, D., and Vladu, A. Towards deep learning models resistant to adversarial attacks. In *ICLR*, 2018.
- Mahloujifar, S., Diochnos, D. I., and Mahmood, M. The curse of concentration in robust learning: Evasion and poisoning attacks from concentration of measure. In *Proceedings of the AAAI Conference on Artificial Intelligence*, volume 33, pp. 4536–4543, 2019.
- Pydi, M. S. and Jog, V. Adversarial risk via optimal transport and optimal couplings. In *Proceedings of the 37th International Conference on Machine Learning*, pp. 7814–7823, 2020.
- Sehwag, V., Mahloujifar, S., Handina, T., Dai, S., Xiang, C., Chiang, M., and Mittal, P. Robust learning meets generative models: Can proxy distributions improve adversarial robustness? In *The Tenth International Conference on Learning Representations, ICLR 2022, Virtual Event, April 25-29, 2022*. OpenReview.net, 2022. URL <https://openreview.net/forum?id=WVX0NNVBBkV>.
- Szegedy, C., Zaremba, W., Sutskever, I., Bruna, J., Erhan, D., Goodfellow, I., and Fergus, R. Intriguing properties of neural networks. *arXiv preprint arXiv:1312.6199*, 2013.
- Tjeng, V., Xiao, K. Y., and Tedrake, R. Evaluating robustness of neural networks with mixed integer programming. In *ICLR*, 2019.

Trillos, N. G., Jacobs, M., and Kim, J. The multimarginal optimal transport formulation of adversarial multiclass classification. *Journal of Machine Learning Research*, 24 (45):1–56, 2023.

Zhang, H., Yu, Y., Jiao, J., Xing, E. P., Ghaoui, L. E., and Jordan, M. I. Theoretically principled trade-off between robustness and accuracy. *arXiv preprint arXiv:1901.08573*, 2019.

A. Proofs

Proof of Lemma 2.2. This follows immediately from Lemma 3.1 with $m = K$. \square

Proof of Lemma 3.1. First, we show that for any $h \in \mathcal{H}_{soft}$, $q_N(h) \leq 1$

We note the first constraint hold because classification probabilities must lie in the range $[0, 1]$. We will now demonstrate that the constraint $B^{\leq m} q \leq 1$ must also hold. For Let $e = ((x_1, y_1), \dots, (x_\ell, y_\ell))$ be a size- ℓ hyperedge in $\mathcal{E}^{(\leq m)}$. By construction of \mathcal{E} , $\exists \tilde{x} \in \bigcap_{i=1}^n N(x_i)$. Also, there is some $S \in \binom{[K]}{m}$ with $\{y_1, \dots, y_\ell\} \subseteq S$. By definition of $q_N(h)$, for each vertex $(x_i, y_i), i \in \{1 \dots n\}$, we have that $q(h)_{(x_i, y_i)} \leq h(\tilde{x}, S)_{y_i}$. Thus,

$$\sum_{i=1}^{\ell} q(h)_{(x_i, y_i)} \leq \sum_{i=1}^{\ell} h(\tilde{x})_{y_i} \leq \sum_{i=1}^K h(\tilde{x})_i = 1.$$

This gives $(Bq)_e \leq 1$.

For any vector q in the polytope, we have a classifier $h : \mathcal{X} \times \binom{[K]}{m} \rightarrow \mathbb{R}^{[K]}$ that achieves at least those correct classification probabilities. This mean that h has the following properties. First, $h(\tilde{x}, L)_y \geq 0$ and $\sum_{y \in [K]} h(\tilde{x}, L)_y = 1$. Second, for all $(x, y) \in \mathcal{V}$, all $\tilde{x} \in N(x)$, and all $L \in \binom{[K]}{m}$ such that $y \in L$, we have $h(\tilde{x}, L)_y \geq q_{(x, y)}$.

To get h , first define the function $g : \mathcal{X} \times \binom{[K]}{m} \rightarrow \mathbb{R}^{[K]}$ so $g(\tilde{x}, L)_y = 0$ for $i \notin L$ and $g(\tilde{x}, L)_y = \max(0, \sup\{q_{(x, y)} : x_y \in \mathcal{V}_y, \tilde{x} \in N(x_y)\})$. Let $L' \subseteq L$ be the set of indicies where $g(\tilde{x}, L)_y > 0$. Then any list of vertices $e = (x_y : y \in L', x_y \in \mathcal{V}_y, \tilde{x} \in N(x_y))$ forms a hyperedge of size $|L'| \leq m$. Thus

$$\sum_{y \in [K]} g(\tilde{x}, L)_y = \sum_{y \in L'} g(\tilde{x}, L)_y = \sup_e \sum_{y \in L'} q_{(x, y)} \leq \sup_e 1 = 1.$$

To produce h , allocate the remaining probability $(1 - \sum_y g(\tilde{x}, L)_y)$ to an arbitrary class. \square

Proof of Lemma 3.3. The first part of this proof applies for any side-information size m . The adversarial strategy for selecting C is a specified by a conditional p.m.f. $p_{C|y}(C|y)$. Thus $p_{y|C}(y|C) = p_{C|y}(C|y)p_{\mathcal{Y}}(y) / \sum_{y'} p_{C|y}(C|y')p_{\mathcal{Y}}(y')$.

The optimal loss of the classifier against a particular adversarial strategy is just a mixture of the optimal losses for each class list: $\sum_C p_{C|y}(C|y) \Pr[p_y(y) L^*(P|(y \in \{i, j\})), N, \mathcal{H}]$.

If $p_{C|y}(C|y) = p_{C|y}(C|y')$ for all $y, y' \in C$, then $p_{y|C}(y|C) = p_{\mathcal{Y}}(y) / \sum_{y' \in C} p_{\mathcal{Y}}(y')$ and the adversary has not provided the classifier with extra information beyond the fact that $y \in C$. Thus $P_{x|y} P_{y|C} = P|(y \in C)$.

Now we can specialize to the $m = 2$ case. Any stochastic matrix s with zeros on the diagonal specifies an adversarial strategy for selecting C with $p_{C|y}(\{i, j\}|i) = s_{i, j}$. Furthermore, if s is also symmetric, $p_{C|y}(\{i, j\}|i) = p_{C|y}(\{i, j\}|j)$ and $p_{y|C}(i|\{i, j\}) = p_{y|C}(j|\{i, j\})$. Then the optimal classifier for the side-information game uses the $\binom{K}{2}$ optimal classifiers for the two-class games and incurs loss $\sum_{i, j} \Pr[Y = i] a_{i, j} s_{i, j}$ where $a_{i, j} = L^*(P|(y \in \{i, j\})), \mathcal{H}, N$. Because the diagonal entries of a are all zero, there is always a maximizing choice of s with a zero diagonal. Thus it is not necessary to include that constraint on s when specifying the optimization. \square

Proof of Lemma 3.4. If $w = 0$, then the lower bound is zero and holds trivially. Otherwise, $\frac{1}{\mathbf{1}^T w} w$ forms a probability distribution over the vertices. Let $X \in \mathcal{V}^{\mathbb{N}}$ be a sequence of i.i.d. random vertices with this distribution. From this sequence, we define a random independent set as follows. Include v in the set if it appears in the sequence X before any of its neighbors in \mathcal{G} . If v and v' are adjacent, at most one of them can be included, so this procedure does in fact construct an independent set. The probability that $X_i = v$ is $\frac{w_i}{\mathbf{1}^T w}$ and the probability that X_i is v or is adjacent to v is $\frac{((A+I)w)_v}{\mathbf{1}^T w}$. The first time that the latter event occurs, v is either included in the set or ruled out. If $w_i > 0$, the probability that v is included in the set is $\frac{w_i}{((A+I)w)_v}$ and otherwise it is zero. Thus the quantity in (6) is the expected size of the random independent set and \mathcal{G} must contain some independent set at least that large. \square

B. Hyperedge Finding

One challenge in computing lower bounds for 0 – 1 loss in the multi-class setting is that we need to find hyperedges in the conflict hypergraph. In this section, we will consider an ℓ_2 adversary: $N(x) = \{x' \in \mathcal{X} \mid \|x' - x\|_2 \leq \epsilon\}$ and describe an algorithm for finding hyperedges within the conflict graph.

We first note that for an n -way hyperedge to exist between n inputs $\{x_i\}_{i=1}^n$, $\{x_i\}_{i=1}^n$ must all lie on the interior of an $n - 1$ -dimensional hypersphere of radius ϵ .

Given input x_1, \dots, x_n where $x_i \in \mathbb{R}^d$, we first show that distance between any two points in the affine subspace spanned by the inputs can be represented by a distance matrix whose entries are the squared distance between inputs. This allows us to compute the circumradius using the distance information only, not requiring a coordinate system in high dimension. Then we find the circumradius using the properties that the center of the circumsphere is in the affine subspace spanned by the inputs and has equal distance to all inputs.

We construct matrix $X \in \mathbb{R}^{d \times n}$ whose i^{th} column is input x_i . Let $D \in \mathbb{R}^{n \times n}$ be the matrix of squared distances between the inputs, i.e., $D_{i,j} = \|x_i - x_j\|^2$.

We first notice that D can be represented by X and a vector in \mathbb{R}^n whose i^{th} entry is the squared norm of x_i . Let $\Delta \in \mathbb{R}^n$ be such vector such that $\Delta_i = \|x_i\|^2 = (X^T X)_{i,i}$. Then given that $D_{i,j}$ is the squared distance between x_i and x_j , we have

$$D_{i,j} = \|x_i\|^2 + \|x_j\|^2 - 2\langle x_i, x_j \rangle,$$

which implies that

$$D = \Delta \mathbf{1}^T + \mathbf{1} \Delta^T - 2X^T X.$$

Let $\alpha, \beta \in \mathbb{R}^n$ be vectors of affine weights: $\mathbf{1}^T \alpha = \mathbf{1}^T \beta = 1$. Then $X\alpha$ and $X\beta$ are two points in the affine subspace spanned by the columns of X . The distance between $X\alpha$ and $X\beta$ is $\frac{-(\alpha - \beta)^T D (\alpha - \beta)}{2}$, shown as below:

$$\begin{aligned} \frac{-(\alpha - \beta)^T D (\alpha - \beta)}{2} &= \frac{-(\alpha - \beta)^T (\Delta \mathbf{1}^T + \mathbf{1} \Delta^T - 2X^T X) (\alpha - \beta)}{2} \\ &= \frac{-(0 + 0 - 2(\alpha - \beta)^T X^T X (\alpha - \beta))}{2} \\ &= \|X\alpha - X\beta\|^2. \end{aligned}$$

Now we compute the circumradius using the squared distance matrix D . The circumcenter is in the affine subspace spanned by the inputs so we let $X\alpha$ to be the circumcenter where $\mathbf{1}^T \alpha = 1$. Let $e^{(i)} \in \mathbb{R}^n$ be the i^{th} standard basis vector. The distance between the circumcenter and x_i is $\|X\alpha - X e^{(i)}\|^2$. From previous computation, we know that $\|X\alpha - X e^{(i)}\|^2 = \frac{-(\alpha - e^{(i)})^T D (\alpha - e^{(i)})}{2}$. Since the circumcenter has equal distance to all inputs, we have

$$(\alpha - e^{(1)})^T D (\alpha - e^{(1)}) = \dots = (\alpha - e^{(n)})^T D (\alpha - e^{(n)}). \quad (7)$$

Note that the quadratic term in α is identical in each of these expressions. In addition, $e^{(i)T} D e^{(i)} = 0$ for all i . So equation 7 simplifies to the linear system

$$\begin{aligned} e^{(i)T} D \alpha &= c \implies D \alpha = c \mathbf{1} \\ &\implies \alpha = c D^{-1} \mathbf{1} \end{aligned}$$

for some constant c . Since $\mathbf{1}^T \alpha = 1$, we have

$$\begin{aligned} 1 &= \mathbf{1}^T \alpha = c \mathbf{1}^T D^{-1} \mathbf{1} \\ \implies \frac{1}{c} &= \mathbf{1}^T D^{-1} \mathbf{1} \end{aligned}$$

assuming that D is invertible. The square of the circumradius, r^2 , which is the squared distance between the circumcenter and x_1 , is

$$\begin{aligned}
 & \|X\alpha - Xe^{(1)}\|^2 \\
 &= \frac{-(\alpha - e^{(1)})^T D(\alpha - e^{(1)})}{2} \\
 &= e^{(1)T} D\alpha - \frac{\alpha^T D\alpha}{2} \\
 &= c - \frac{c^2 \mathbf{1}^T D^{-1} \mathbf{1}}{2} \\
 &= \frac{c}{2} \\
 &= \frac{1}{2\mathbf{1}^T D^{-1} \mathbf{1}}.
 \end{aligned}$$

Therefore, assuming matrix D is invertible, the circumradius is $\frac{1}{\sqrt{2\mathbf{1}^T D^{-1} \mathbf{1}}}$.

The inverse of D can be computed as $\frac{\det D}{\text{adj } D}$. Since $\alpha = cD^{-1}\mathbf{1}$, we have $\alpha = c\frac{\det D}{\text{adj } D}\mathbf{1}$. As $r^2 = \frac{c}{2}$, constant c is non-negative. Therefore, $\alpha \propto \frac{\det D}{\text{adj } D}\mathbf{1}$.

When all entries of α are non-negative, the circumcenter is a convex combination of the all inputs and the circumsphere is the minimum sphere in \mathbb{R}^{n-1} that contains all inputs. Otherwise, the circumsphere of $\{x_i | \alpha_i > 0\}$ is the minimum sphere contains all inputs.

After finding the radius of the minimum sphere that contains all inputs, we compare the radius with the budget ϵ . If the radius is no larger than ϵ , then there is a hyperedge of degree n among the inputs.

C. Experimental Setup

Datasets We compute lower bounds for MNIST (LeCun & Cortes, 1998), CIFAR-10, and CIFAR-100 (Krizhevsky & Hinton, 2009). Since we do not know the true distribution of these datasets, we compute lower bounds based on the empirical distribution of the training set for each dataset.

Attacker We will consider an ℓ_2 adversary: $N(x) = \{x' \in \mathcal{X} | \|x' - x\|_2 \leq \epsilon\}$. This has been used in most prior work (Bhagoji et al., 2019; Pydi & Jog, 2020; Trillos et al., 2023).

LP solver For solving the LP in Equation 4, we primarily use Mosek LP solver (ApS, 2019). When Mosek solver did not converge, we use CVXOpt’s LP solver (Andersen et al., 2013).

Training Details For MNIST, we use 40 step optimization to find adversarial examples during training and use step size $\frac{\epsilon}{30}$ and train all models for 20 epochs. For CIFAR-10 and CIFAR-100, we use 10 step optimization to find adversarial examples and step size $\frac{\epsilon}{7}$ and train models for 100 epochs. For MNIST TRADES training, we use $\beta = 1$ and for CIFAR-10 and CIFAR-100, we use $\beta = 6$. Additionally, for CIFAR-10 and CIFAR-100, we optimize the model using SGD with learning rate and learning rate scheduling from Gowal et al. (2020). For MNIST, we use learning rate 0.01.

Architectures used For CIFAR-10 and CIFAR-100, we report results from training a WRN-28-10 architecture. For MNIST, we train a small CNN architecture consisting of 2 convolutional layers, each followed by batch normalization, ReLU, and 2 by 2 max pooling. The first convolutional layer uses a 5 by 5 convolutional kernel and has 20 output channels. The second convolutional layer also uses a 5 by 5 kernel and has 50 output channels. After the set of 2 convolutional layers with batch normalization, ReLU, and pooling, the network has a fully connected layer with 500 output channels followed by a fully connected classifier (10 output channels).

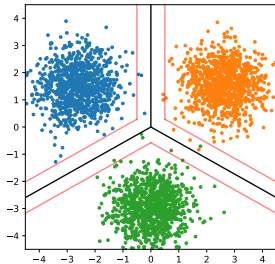
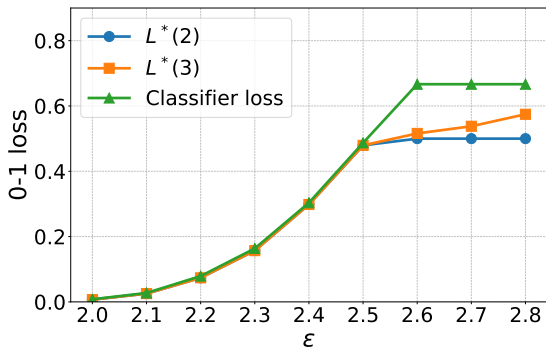
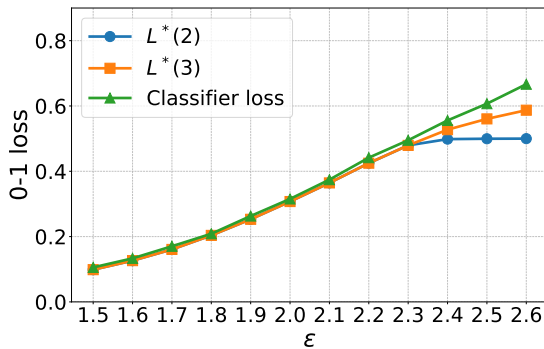


Figure 5: A sample 3-class Gaussian problem (each color pertains to a class) and a corresponding classifier for this problem shown in black. The classifier classifies a sample incorrectly when it lies over the edge of the ϵ margin (shown by the red lines) nearest the corresponding Gaussian center.



(a) $\sigma^2 = 0.05$



(b) $\sigma^2 = 0.5$

Figure 6: Lower bounds on error for the Gaussian 3-class problem ($\sigma^2 = 0.05$ and $\sigma^2 = 0.5$) computed using only constraints from edges ($L^*(2)$) and up to degree 3 hyperedges ($L^*(3)$) in comparison to the performance of the deterministic 3-way classifier depicted in Figure 5.

D. Additional Experimental Results

D.1. Results for Gaussian data

We begin with a 3-way classification problem on 2D Gaussian data. To generate our Gaussian dataset, we sample 1000 points per class from 3 spherical Gaussians with means at distance 3 away from the origin (a sample is shown in Figure 5). We compute multiclass lower bounds via the LP in Lemma on robust accuracy at various ℓ_2 budget ϵ and display these values in Figure 6 as $L^*(3)$. Additionally, we compare to a deterministic 3 way classifier. This classifier is the best performing out of the 2 strategies: 1) constantly predict a single class (thus achieving $\frac{2}{3}$ loss) or 2) is the classifier in black in Figure 5 which classifies incorrectly when a sample lies over the edge of the nearest ϵ margin of the classifier.

We observe that at smaller values of ϵ , the loss achieved by the 3-way classifier matches optimal loss ($L^*(3)$); however, after $\epsilon = 2.5$ for $\sigma^2 = 0.05$ and $\epsilon = 2.3$ for $\sigma^2 = 0.5$, we find the classifier no longer achieves optimal loss. This suggests that there is a more optimal classification strategy at these larger values of ϵ . In Figures 7 and 8, we visualize the distribution of correct classification probabilities obtained through solving the LP with and without considering hyperedges. These figures are generated by taking a fresh sample of 1000 points from each class and coloring the point based on the correct classification probability q_v assigned to its nearest neighbor that was used in the conflict hypergraph when computing the lower bound. We observe from Figure 7, for all classes, the data are mostly assigned classification probabilities around 0.5. In Figure 8, we can see that when we consider hyperedges, we some of these 0.5 assignments are reassigned values close to $\frac{2}{3}$ and $\frac{1}{3}$. Interestingly, we notice that when we do not consider hyperedges, our solver finds an asymmetric solution to the problem (strategies for class 0, 1, and 2 differ) while when considering hyperedges this solution becomes symmetric.

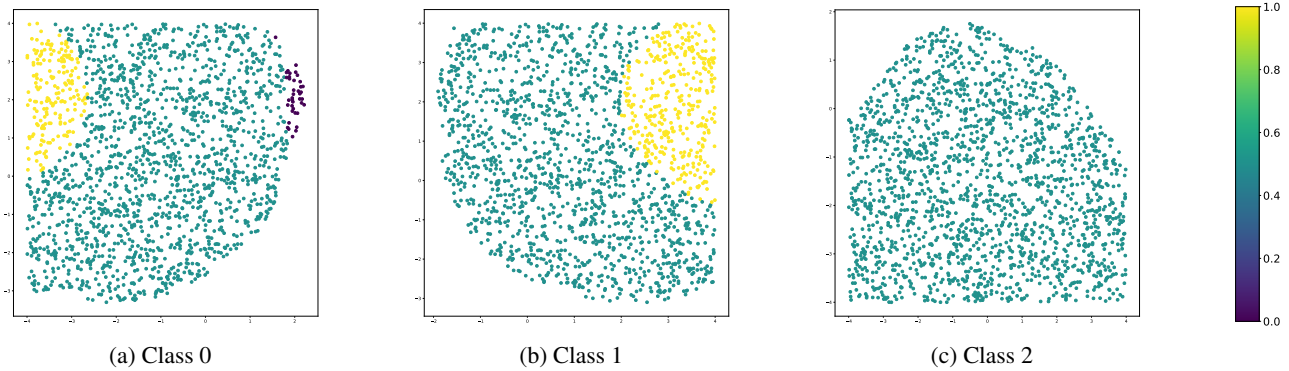


Figure 7: Distribution of optimal classification probabilities across samples from each class of the Gaussian obtained as a solution when computing $L^*(2)$.

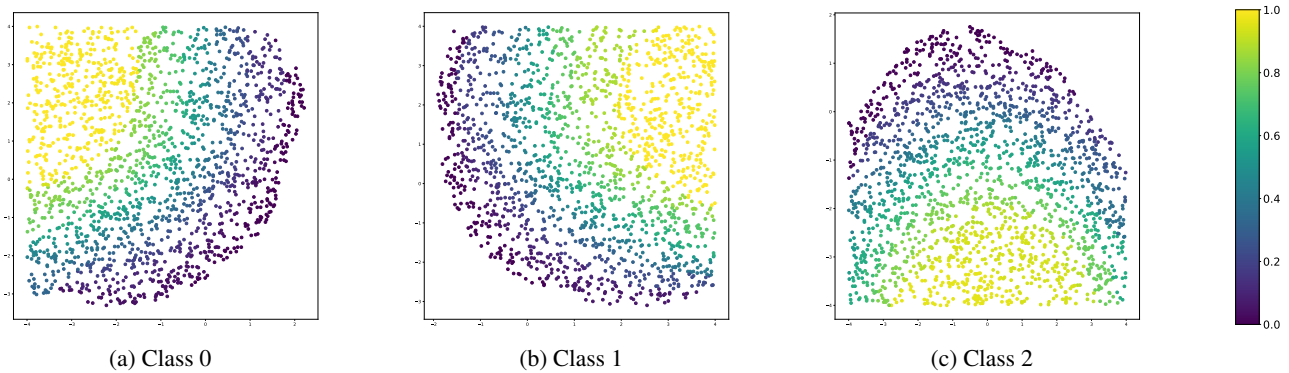


Figure 8: Distribution of optimal classification probabilities across samples from each class of the Gaussian obtained as a solution when computing $L^*(3)$.

D.2. Additional adversarial training results

In Figure 9, we also add the loss achieved by PGD adversarial training. We find that this approach generally performs worse on MNIST compared to TRADES and is also unable to fit to CIFAR-10 data at the ϵ values tested.

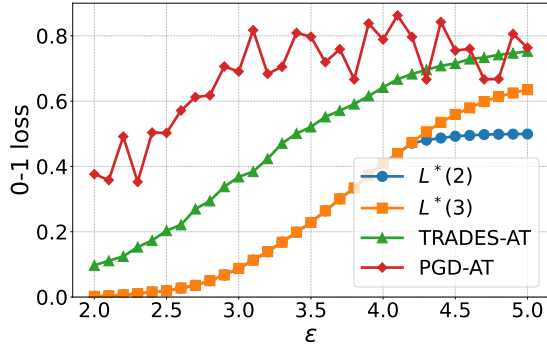
D.3. Truncated hypergraph lower bounds for CIFAR-100

We provide results for truncated hypergraph lower bounds for the CIFAR-100 train set. We observe that similar to MNIST and CIFAR-10, including more hyperedge constraints does not influence the computed lower bound.

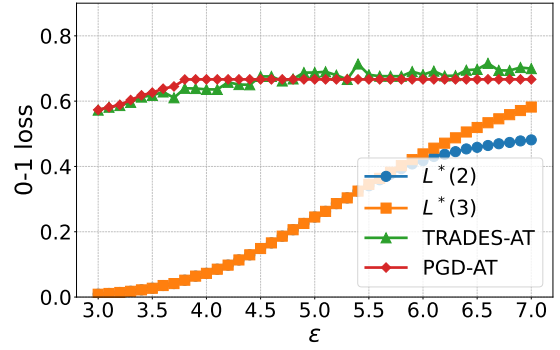
D.4. Impact of hyperedges

In Figure 11, we show the count of edges, degree 3 hyperedges, and degree 4 hyperedges found in the conflict hypergraphs of the MNIST, CIFAR-10, and CIFAR-100 train sets. We note that we did not observe any increase in loss when considering degree 4 hyperedges at the ϵ with a data point for number of degree 4 hyperedges in Figure 11. We find that the relative number of edges and hyperedges is not reflective of whether we expect to see an increase in loss after considering hyperedges. For example in CIFAR-10, at $\epsilon = 4.0$, we there are about 100 times more hyperedges than edges, but we see no noticeable increase in the 0 – 1 loss lower bound when incorporating these hyperedge constraints.

Similar to Figure 4 in the main body of the paper, we plot the distribution of vertex weights q_v obtained through solving the LP for $L^*(2)$ and $L^*(3)$ for CIFAR-10 in Figure 12. Similar to trends for MNIST, we find that the gap between $L^*(2)$ and $L^*(3)$ only occurs when the frequency of 0.5 weights is higher.



(a) MNIST (1, 7, 9)



(b) CIFAR-10 (0, 2, 8)

Figure 9: Lower bounds on error for MNIST and CIFAR-10 3-class problems (1000 samples per class) computed using only constraints from edges ($L^*(2)$) and up to degree 3 hyperedges ($L^*(3)$) in comparison to TRADES adversarial training (TRADES-AT) and PGD adversarial training (PGD-AT) loss.

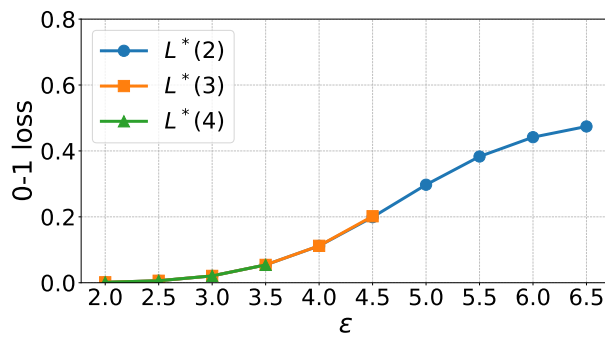


Figure 10: Lower bounds for optimal 0-1 loss the for CIFAR-100 train set

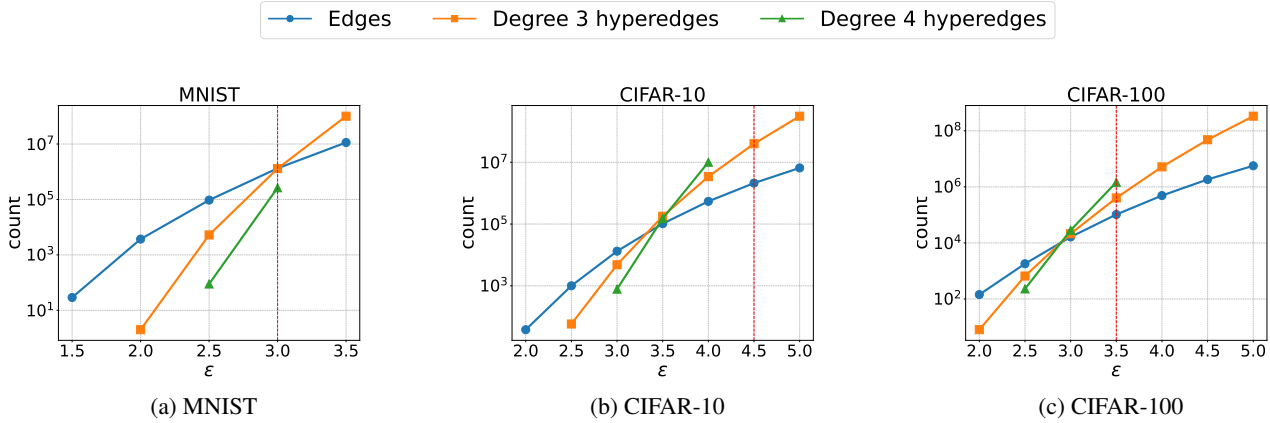


Figure 11: Number of edges, degree 3 hyperedges, and degree 4 hyperedges found in the conflict hypergraphs of MNIST, CIFAR-10, and CIFAR-100 train sets. The red vertical line indicates the ϵ at which we noticed an increase in the 0 – 1 loss lower bound when considering degree 3 hyperedges.

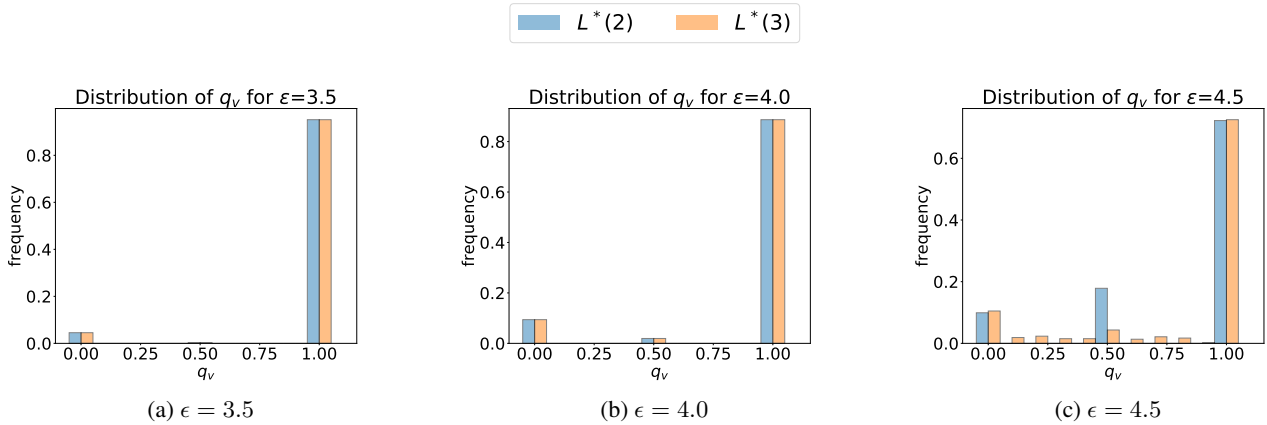


Figure 12: Distribution of optimal classification probabilities q obtained by solving the LP with up to degree 2 hyperedges ($L^*(2)$) and up to degree 3 hyperedges ($L^*(3)$) on the CIFAR-10 training set.

D.5. Computational complexity of computing lower bounds

Our experiments of $L^*(3)$ for higher ϵ are limited due to computation constraints. Figure 13 we see that the time taken to compute the losses grows rapidly with ϵ . In future work, we are seeking algorithmic optimization to achieve more results at high ϵ .

D.6. Pairwise optimal losses for 1v1 binary classification problems

In Section 4.2, we computed a lower bound on loss from maximum weight coupling over optimal losses for 1v1 binary classification problems. In Figure 14, we show the heat maps for optimal losses for each pair of 1v1 classification problems for $\epsilon = 3$ on MNIST and $\epsilon = 4$ on CIFAR-10. We find that for both datasets only a few pairs of classes have high losses. Specifically, for MNIST, we find that the class pairs 4-9 and 7-9 have significantly higher loss than all other pairs of classes. For CIFAR-10, we find that 2-4 has the highest loss compared to other pairs, and 2-6 and 6-4 are also quite high.

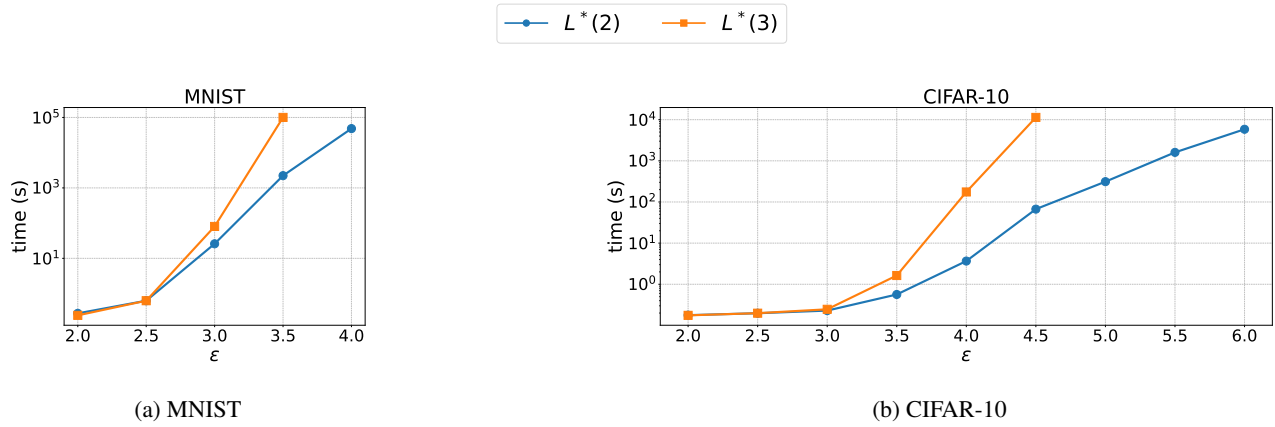


Figure 13: Time taken to compute $L^*(2)$ and $L^*(3)$ for MNIST and CIFAR-10.

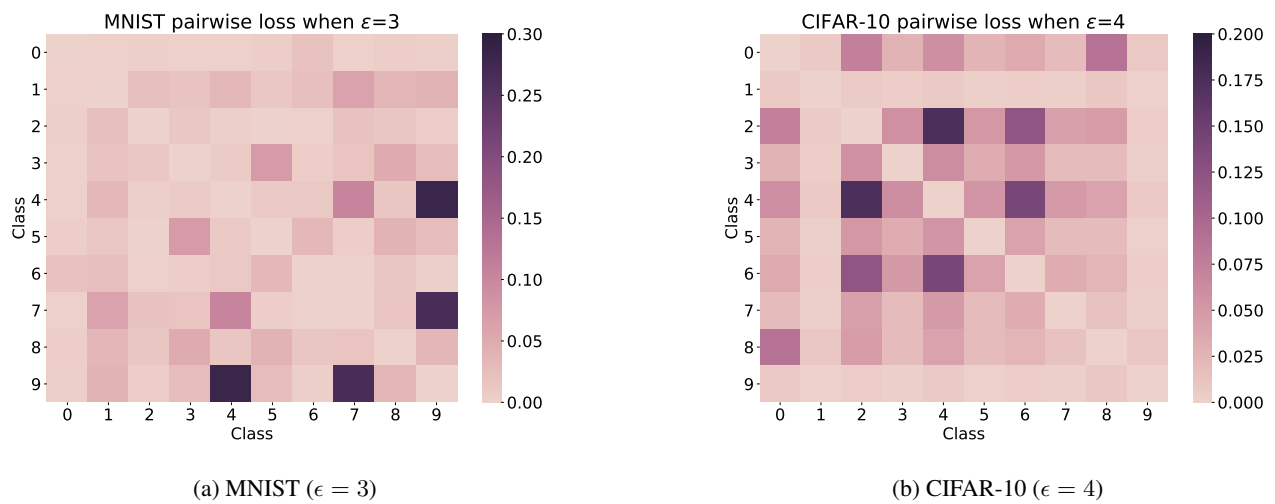


Figure 14: Heat maps for optimal loss for each pair of 1v1 classification problems.